

Multispectral Imaging with Raspberry Pi for Assessment of Plant Health Status

JAN LUKAS BOSSE

Georg August Universität Göttingen
janlukas.bosse@stud.uni-goettingen.de

MARCELINUS A. S. ADIWIBAWA

Universitas Machung
marcelinus.setya@machung.ac.id

TATAS H. P. BROOTOSUDARMO

Universitas Machung
tatas.brotosudarmo@machung.ac.id

September 30, 2016

Abstract

Non-destructive measurement of plant chlorophyll concentration using the normalized difference vegetation index (NDVI) has long been standard practice to determine the plant health status. This is, because the NDVI value is correlated with the chlorophyll concentration which in turn is highly correlated with other vital plant parameters such as nitrogen and magnesium concentration. Initially the NDVI values were obtained from satellite imagery and thus could only be used to assess the health status of bigger ecosystems like forests and crop fields. With the introduction of handheld chlorophyll meters like the Chlorophyll Meter SPAD-502 Plus made by Konica Minolta, the same principle could be used to determine the chlorophyll concentration of single leaves. However these devices still have one major shortcoming: They can only measure the chlorophyll concentration on one single spot on the leaf at a time. But depending on the species the chlorophyll concentration tends to vary significantly over the leaf. To overcome this shortcoming, we developed our PlantAnalyzer which offers better spatial resolution of the NDVI values and hence the chlorophyll concentration. Its technical realization and precision shall be elaborated in the following article.

I. INTRODUCTION

Chlorophyll concentration is an important parameter to monitor the physiological status of plants. Chlorophyll concentration is controlled by the availability of nutrients such as nitrogen, magnesium, iron, calcium, manganese and zinc, as was shown by Bottrill, Possingham, and Kriedemann [2] and thus gives information about nutrient deficiencies or costly over fertilization. The most common method to check the plant health status is the N-Kjeldahl test for measuring nitrogen concentration [5]. Another *in vitro*-method are the spectrophotometric methods developed by Lichtenthaler [6] and Porra, Thompson, and Kriedemann [9] to analyze chlorophyll extracts from a leaf sample. However these methods are destructive, very time consuming and expensive.

To overcome these disadvantages optical methods based on the reflectance spectrum of chlorophyll have been developed. One of the most popular ones is the *normalized difference vegetation index (NDVI)* index, which uses the fact that vegetation has a high reflectance in the near infrared part of the spectrum but a rather low reflectance in the red band. The NDVI value represents exactly this difference in reflectance [14]:

$$NDVI = \frac{IR - R}{IR + R} \quad (1)$$

where *IR* and *R* stand for the reflectance in the near infrared and red band respectively. The reflectance curves of green and yellow *Manihot esculenta* (cassava) leaves are shown in Figure 1.

The *soil plant analysis development value (SPAD)* can be measured with handheld chlorophyll me-

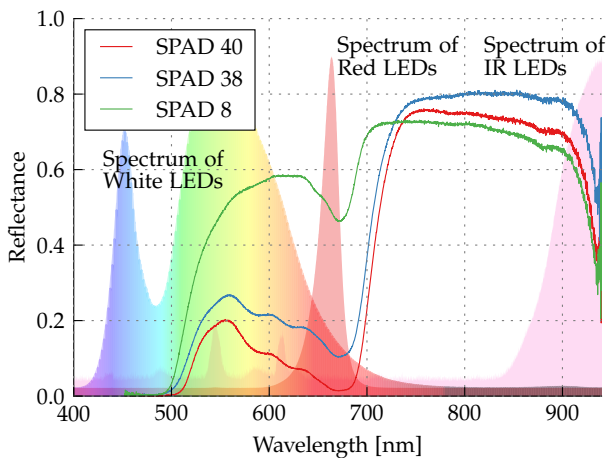


Figure 1: Reflectance spectrum of cassava leaves with different SPAD values together with the emission spectra of the LEDs used. It is clearly visible, that for higher SPAD values the ratio between the reflectance in the infrared band and the red band is also higher. Higher SPAD values correspond to healthier, i.e. greener leaves. The data was obtained using a Ocean Optics USB4000 spectrometer.

ters like the SPAD-502. They also makes use of this difference in reflectance by shielding the region of interest (ROI) from outside light and shining red and near infrared light through the specimen to measure the absorption rate [8]. While this has the advantage of a simple hand held device which can be used *in situ*, it is limited to measuring the chlorophyll content of a ca. 3 mm^2 ROI and is not particularly accurate with thicker leaves, where the absorption is almost 1 for both the near infrared and the red band.

Our *PlantAnalyzer* complements these devices by calculating the pixel-wise NDVI value from two images where the plant was illuminated with red light in one image and with near infrared light in the other image (see Figure 3). The result is a chlorophyll concentration color index/heatmap which not only reflects the average chlorophyll concentration in the specimen, but also the distribution within the specimen.

It can be shown that the anthocyanin concentration in plant tissue is correlated with the ratio of reflectance in the red and green band [see 13, 7].

Thus we included the calculation of the red/green ratio in our analysis and displayed in the same way as the NDVI values.

Thus the red/green ratio is defined as

$$RG = \frac{R}{G} \quad (2)$$

where R and G are the reflectances in the red and green band respectively.

As additional information our *PlantAnalyzer* also calculates an estimate of the total leaf area and the average NDVI value and R/G-ratio of the leaves.

II. METHODS

i. System Overview

The main idea for the *PlantAnalyzer* was to create a controlled environment, in the sense that the lighting conditions can be manipulated freely and the background color is known. This should allow more precise measurement of the NDVI value and R/G ratio, than the values obtained from satellite imagery or *in situ* under varying lighting conditions.

An analysis chamber with high power LEDs of three different wavelenghts as light sources was built. It also included two Raspberry Pi 3 units to control the LEDs and do all the computing work. One of the Raspberry Pi units is equipped with an ordinary RGB camera module while the second one is equipped with the infrared camera module¹. The *PlantAnalyzer* takes four different pictures of the plant. First a stereo image pair is taken with the white LEDS turned on. Then one picture with the red LEDs turned on and one with the IR LEDs turned on are taken. These pictures are then analyzed to obtain the NDVI values and R/G ratios from the red and the IR pictures and the RGB picture respectively. From these values we calculate a chlorophyll concentration heatmap as well as a R/G ratio heatmap for easier evaluation

¹Actually the IR camera is just an ordinary RGB camera without the IR filter, and thus perfectly able to capture normal RGB images, if the light source does not emit much light in the IR part of the spectrum

of the results. The RGB images are also used to section the images, i.e. separate the leaves from the background, and to calculate a depth map of the plant. To do so the disparity of one point is calculated from which the distance of the point from the camera can be estimated. Using this depth map we also calculate an estimate of the total leaf area as well as a normalized average of the NDVI values.

All these results are presented in a graphical user interface (GUI) which makes it possible to see the chlorophyll distribution and R/G values at a glance and also print the exact NDVI values or R/G-ratios of interesting pixels to the screen by clicking on them. The GUI also allows the user to save the whole set of images and load old sets for comparison.

To verify our obtained NDVI-values and calibrate them to actual chlorophyll concentrations we compared them with the SPAD values measured with our SPAD-502 meter, whose characteristics with different species and also plant independent chlorophyll concentration curves are well studied.

The results from Mark R. Steele and Merzlyak [7] and Sims and Gamon [13] suggest that it is possible to find a correlation between the RG ratios and anthocyanin concentration, but that this correlation is dependent on the species and the chlorophyll concentration. Since because the chlorophyll concentration can be estimated from the NDVI value this factor is known and taking it into consideration for anthocyanin concentration estimations should make them more robust.

ii. Hardware

The PlantAnalyzer consists of an analyzation chamber with different light sources and two Raspberry Pi units with a camera unit each. The analyzation chamber is made from non-transparent with acrylic sheets for the walls and aluminium bars as edges. Its dimensions (height \times width \times depth) are $100 \times 50 \times 50$ cm and the cameras and LEDs are mounted at approximately 75 cm height.

The heart of the PlantAnalyzer are the two aforementioned Raspberry Pi units. The first one is

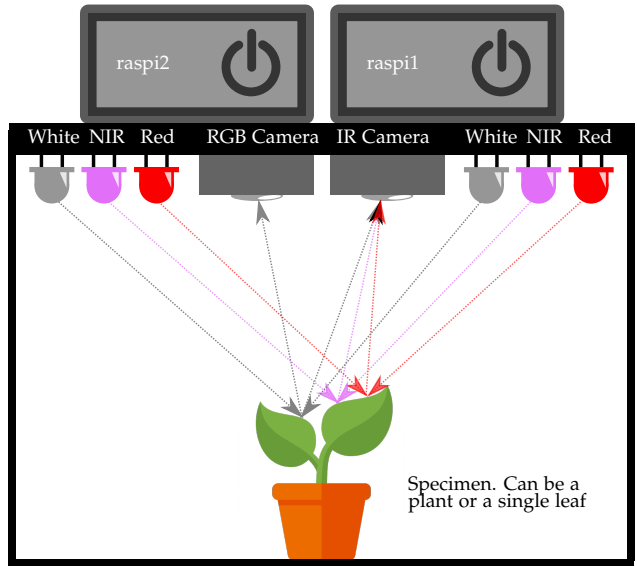


Figure 2: Sketch of the PlantAnalyzer. Each of the LED arrays consists of three high power LEDs, making it a total of 18 LEDs. The cameras are approximately 3 cm apart, which makes them suitable for stereo vision. The sketch is not to scale

equipped with the Raspberry Pi NoIR v1 camera module while the second one is equipped with the Raspberry Pi camera v1 module. The sole purpose of the second Raspberry Pi is to control the second camera unit and then send the captured images via ssh to the first Raspberry Pi. This first one is responsible for all the heavy computing work, including image arithmetics and analysis and displaying the GUI.

As light sources we have two sets of three 3W high power LEDs per color. For sectioning purposes and to calculate the disparity map and thus depth information the first Array of LEDs consists of white LEDs. The second and third Array consist of Red and near infrared LEDs with 660 nm and 940 nm wavelength respectively, the exact emission spectra are shown in Figure 1. The red and infrared LEDs are used to illuminate the two pictures needed to calculate the NDVI values. All LED arrays are arranged symmetrically around the cameras, as shown in Figure 2. The LEDs are driven by affordable china made LED-Drivers ²

²<https://www.tokopedia.com/tanakazyo/driver-high-power-led-3x-3w-or-1x-10w-ac-dc-mr16>

whose power supply is controlled using the *general purpose in and output ports (GPIO)* of the main Raspberry Pi and some standard Darlington transistors. For the schematics see A.vii.

The 50 Hz flickering in the brightness of the LEDs within one exposure was taken into account by adding a vertical (in the resulting images) grey calibration bar inside of the analyzation chamber. To correct the flickering the exact flickering curve along a column is quantified using the brightness values of this calibration bar and this flickering curve is then used to "deflicker" the image by software. Details on the technique used and goodness of it can be found in Chapter A.v.

iii. Software and Algorithms

Almost all software for the image analysis was written using Python and the popular opencv and numpy libraries which provide image analyzation and array manipulation functionality for python using native C/C++-code in the backend, making them very efficient in both the coding and computing time. The GUI was written using the PyGTK Python bindings of GTK and using the GUI designer Glade.

The analyzation process consists of 7 main steps:

- First the images must be **deflickered** to correct the bars of different brightness caused by the flickering light sources. The exact algorithm used is described in section A.v.
- Then the images are **undistorted**. opencvs stereoSGBM algorithm, which is used to calculate the disparity map, works only with perfectly aligned images where one point in the right picture is in exactly the same line in the left picture. Since our two cameras are not that perfectly aligned and also do not perfectly satisfy the assumptions of a pinhole camera model the images have to be undistorted using opencvs initUndistortRectifyMap and remap functions. The distortion parameters were determined using the strategy described in [11].
- After that the pixel wise **NDVI values** are calculated according to (1). For the reflectance in

the near infrared band *IR* and in the red band *R* we used the pixel values of the red channel of the images taken under near infrared and red illumination respectively, because those pixel values are – up to scale and eventually the application of tonal response curves – the same as the radiances used by Tucker [14] in his original work. The exposure times for both images were chosen such that we would get the maximum possible dynamic range for both images, i.e. the pixel value 255 for white paper and 0 for black paper. Given the standard deviation in the calculated NDVI value of one single leaf (see section III) this dynamic range is more than sufficient.

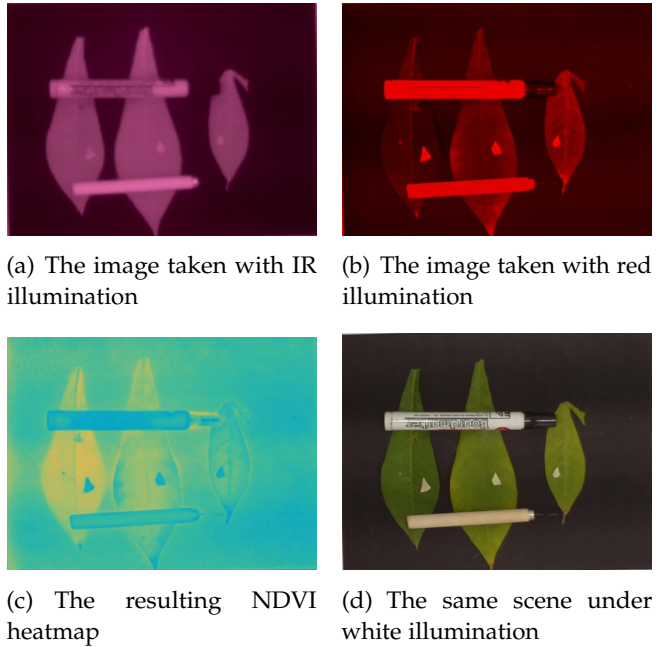


Figure 3: Overview over the calculation of the NDVI values. After calculating the pixelwise NDVI value as in (1) from the red channels of the images and rescaling the domain [-1,1] to [0,255] the colormap *parula* is applied to make subtle changes in the NDVI values better visible. These are not the full images as taken by the Raspberry Pi cameras, but only cropped versions to show the most interesting region. The images were taken from the calibration data sets and show three cassava leaves with different SPAD values, as can be seen in the NDVI heatmap.

- Similarly the pixel wise **R/G ratio** are calculated according to (2). As values for R and G we used the pixel values of the red and the green channel of the RGB images (under white illumination). To visualize the R/G ratios in a useful way, the histogram of the ratios is equalized. For details about the equalization formula see A.vi.
- In the next step we **mask the leaves** to do the calculations for the average NDVI value and the leaf area only on pixels, that actually show leaves. For the mask it was sufficient to simply select pixels whose saturation was over a certain threshold in the RGB images, because the interior of the PlantAnalyzer is completely white and appears in different shades of grey in the RGB image.
- Now the **disparity map** is calculated from the undistorted RGB images from the right and the left camera. Again we trusted the magic of opencv's inbuilt functions and proceeded as described in [10] using the stereoSGBM algorithm and our own empirically determined parameters.
- Last the **average NDVI value, average R/G ratio and a leaf area estimate** are calculated. For the leaf area estimate we calculate the pixel wise area per pixel value as described in A.iv and then sum over all pixels that were identified displaying leaves in the masking process. For the weighted average NDVI value we multiply these area per pixel values by the NDVI value of the corresponding pixel, sum over all pixels displaying leaves and then divide by the leave area estimate. This strategy ensures that the average is adjusted for the fact that leaves which are closer to the camera span more pixels in the image. The same goes for the average R/G ratio.

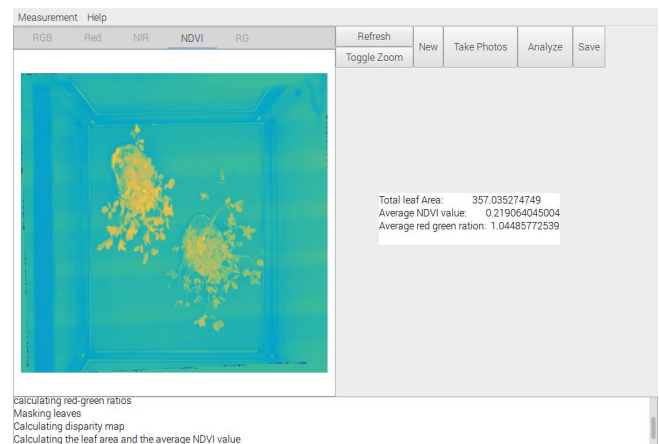
All important results are then displayed in the GUI of the PlantAnalyzer program.

iv. Workflow

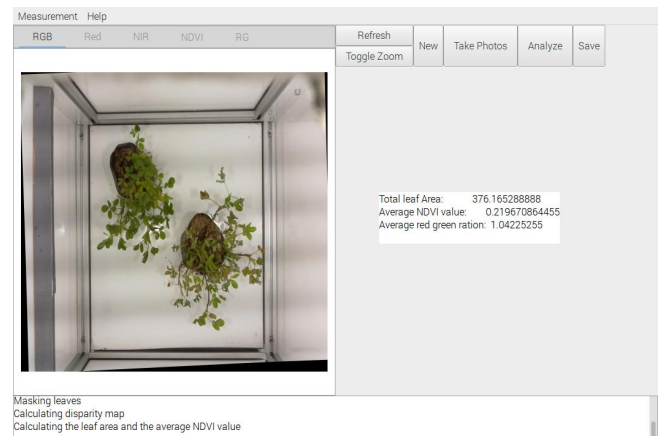
In the following the normal workflow, where the user just wants to analyze one single plant, is de-

scribed.

After placing the plant in the analyzation chamber and closing it, so that no external light can enter the chamber the user can set the project name using the *New* Button in the GUI. After that the images are taken by clicking the *Take Photos* button. Now the RGB image taken with the left camera as well as the red and the near infrared image are already visible in the GUI and may be inspected, whether the whole ROI was captured and the calibration bar is not covered by leaves (!).



(a) The view of the NDVI heatmap



(b) The view of the photos under white illumination

Figure 4: Screenshots of the PlantAnalyzer GUI

After the images are taken, which is signaled by the message "Right Photo retrieved" in the log window on the bottom of the GUI, one may press the *Analyze* button which invokes the analyzation process. This analyzation process takes up to two

minutes to finish on the Raspberry Pi, because it includes some quite computing intensive work like calculating the disparity map and the pixel wise NDVI value on a 5 MP image. The current step of the analyzation is shown in the log window on the bottom of the window.

Once the analysis is done the results for the estimated leaf area and the average NDVI value and average R/G ratio are displayed in the result panel on the right side of the screen. To obtain the exact NDVI values or R/G ratios of different spots on the leaf it is possible to left-click on them in the respective heat map view. Then the value of the clicked pixel is written to the log window. For more precise selection of the spot, it is possible to toggle between a fitted view and a 100% view of the heatmaps using the *Toggle Zoom* button.

For later analyzation or comparison with other specimens it is possible to save the whole set of images via *Measurement -> Save* to the current project name or via *Measurement -> Save as* to a name of your choice. These zip-Files can later be opened via *Measurement -> Open* or by starting the PlantAnalyzer with the option `-f filename.zip`. Note however, that they typically take up to 6 MB of your valuable hard drive space.

The measurement class is a module independent of the GUI which means any technical interested and versed person can use it to write his own analyzation scripts for e.g. time-lapse analysis of leaf senescence and extract even more data from the images such as an estimate of the average leaf size. The source code and a detailed documentation are available at [1].

III. RESULTS

i. NDVI and SPAD values

The calibration of our PlantAnalyzers NDVI values to actual chlorophyll concentrations was done using the SPAD-502 as a intermediate step. Twelve different cassava leaves with different SPAD values (as measured with the SPAD-502) ranging from 0.6 to 40 were selected from the fields of Universitas Ma Chung. For each of these leaves one point was

marked using tape and then scanned four times with both, the SPAD-502 chlorophyll meter and with the PlantAnalyzer. Since the cassava leaves are to a certain degree transparent to near infrared and red light, which is why the SPAD-502 works at all, the measured NDVI-values differ depending on the background. Thus we decided to scan the leaves twice with the PlantAnalyzer: Once with a white background, which reflects the situation where one wants to analyze a single loose leave, and once with black background which reflects the situation, where one wants to analyze leaves which are still attached to a plant and thus hang freely without something behind them to reflect light. Some of the sample pictures can be found in the appendix A.iii.

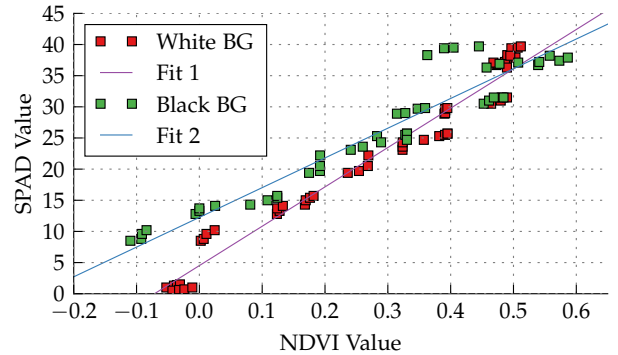


Figure 5: Linear Regression between the measured NDVI values and the SPAD values from the SPAD-502 chlorophyll meter. The red data points are those, where the NDVI values were calculated from images with a white background, while the green data points are those where a black background was used. This color scheme is used throughout all following plots.

The results are presented in Figure 5 and Table 1 and show that the NDVI values of the cassava leaves obtained with the PlantAnalyzer correlate well with the values from the SPAD meter in the range from 0 to 35. From 35 upwards the correlation is not as good as before.

Verification

To further verify these findings we got another set of ten leaf samples and used the results from the linear regression to predict the SPAD values from

	White Background	Black Background
a	63.2 ± 3.5	47.4 ± 3.1
b	4.5 ± 1.2	12.3 ± 1
r^2	0.9656	0.9519
p	$2.9 \cdot 10^{-34}$	$1.3 \cdot 10^{-34}$

Table 1: Overview over the results of the regression analysis. a and b are the values for slope and intercept of the linear regression curve while r^2 and p are the coefficient of determination and the two sided p -value for the null hypothesis test. For the standard deviations the square-roots of the diagonals of the covariance matrix were used.

the NDVI values measured with the PlantAnalyzer. For each leaf we marked one to two spots on the leaf with tape and for each of the spots we measured both the NDVI and the SPAD value four times, to deal with the fact, that the NDVI and the SPAD values tend to change quickly even on small length scales. As before we measured the NDVI value twice, once with a black background and once with a white background. The results are shown in Figure 6.

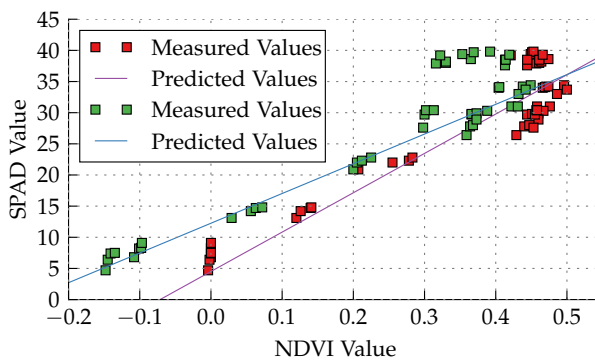


Figure 6: Comparison of the measured SPAD values and the SPAD values predicted from the NDVI values. Again red was used for the values obtained from images with a white background and green for values, where we had a black piece of paper behind the leaves as a background.

Once again one can see, that the PlantAnalyzer works well to predict SPAD values in the range from 0 to 35, but is not as precise from 35 upwards. This was to be expected considering the results from Figure 5.

ii. Correlation of SPAD values and chlorophyll concentration

To predict the actual the chlorophyll concentration from the NDVI values the SPAD values had to be correlated with the chlorophyll concentration. This work was done as part of a different project at the *Ma Chung Research Center for Photosynthetic Pigments (MRCPP)* by Evan Hutomo E.P. using cassava leaves with a wide range of different SPAD values. The chlorophyll concentration was determined using the method developed by Lichtenthaler [6] using 100% acetone as a solvent.

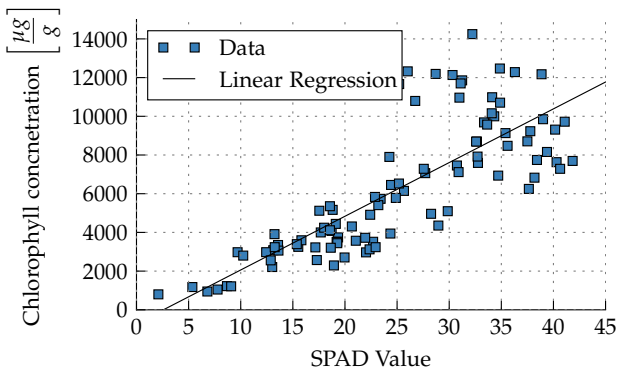


Figure 7: Linear Regression between the measured SPAD values and the chlorophyll concentration in cassava leaves.

Parameters of the linear Regression	
a	278 ± 21
b	-720 ± 570
r^2	0.6399
p	$8.7 \cdot 10^{-23}$

Table 2: Overview over the results of the regression analysis. a and b are the values for slope and intercept of the linear regression curve while r^2 and p are the coefficient of determination and the two sided p -value for the null hypothesis test. For the standard deviations the square-roots of the diagonals of the covariance matrix were used.

Combining the results from Table 1 and Table 2 we get our final formula for estimating the chlorophyll concentration from the NDVI values:

White Background

$$CC(NDVI) = 17500 \cdot NDVI + 540$$

with the standard deviation estimate

$$\sigma_{CC} = \sqrt{(\sigma_{NDVI} \cdot 17500)^2 + (NDVI \cdot 1700)^2}$$

Black Background

$$CC(NDVI) = 13200 \cdot NDVI + 2700$$

with the standard deviation estimate

$$\sigma_{CC} = \sqrt{(\sigma_{NDVI} \cdot 13200)^2 + (NDVI \cdot 1300)^2}$$

Where CC stands for *chlorophyll concentration* and σ_i for the respective standard deviation. The formulas for the standard deviation have been derived according to the rules of linear error propagation using the standard deviations from the regression parameters shown in Tables 1 and 2.

iii. Leaf Area estimation and average NDVI value

To determine the margin of error for the leaf area estimate and average NDVI value and find their dependence on the distance from the camera and light sources we ran two more tests. For the first one single cassava leaves that lied flat on a white surface were used while for the second one a young *Arachis pintoi* plant, whose leaves would overlap each other and were not always orthogonally facing the camera, was used. For both test objects we made 7 measurements in different heights and, in the case of the plant, different orientations. In each case the average NDVI value, the leaf area estimate and the typical disparity value on a leaf as calculated by our software were written down.

The results of these tests are presented in Figure 8 and 9. It is clearly visible that both the leaf area estimate as well as the average NDVI value estimate work better, if the plant is further away from the cameras and light sources. If the plant is too close to cameras and light sources the illumination of the leaves depends too much on their position in the xy-Plane and the calculation of the disparity map fails, resulting in a unusable disparity map

and NDVI values that are not consistent in the xy-Plane.

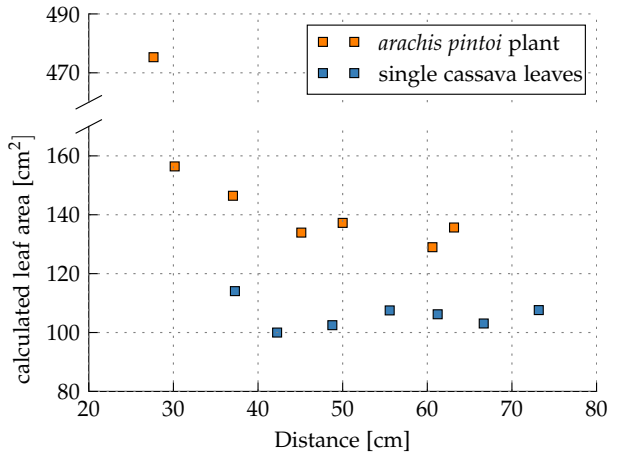


Figure 8: The dependence and variations of the calculated leaf area estimate. The outlier at the very end of the *Arachis pintoi* plant data is caused by the wrong disparity map for extremely high disparities. This resulted in unrealistically high area per pixel values. Thus it was ignored in the further analysis.

If the camera has a planar view of the leaves and they do not cover each other the estimation of the leaf area from the depth map and the pixel counting works well, as can be seen from Figure 8. However if the object of interest is not a leave, but a whole plant the estimated leaf area varies more, depending on the orientation of the plant and distance from the camera.

Interestingly the dependence of the average NDVI value from the distance from the camera depends not only on the orientation of the leaves, but also on the species. While the average NDVI value was more or less constant over the whole range for the *Arachis pintoi* plant, it decreased with the distance for the cassava leaves. This means, that it is neccessary to have different calibration curves for different species and that the calibration curves also depend on the distance from the cameras and light sources.

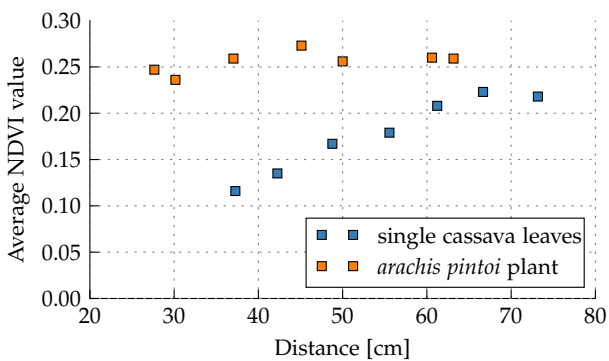


Figure 9: The dependence and variations of the calculated average NDVI value. Interestingly the average NDVI value is dependent on the distance from the light sources for cassava leaves, but not for the *Arachis pinto* plant

IV. DISCUSSION

While the calibration curves from section III.i give good results for cassava leaves in a well defined distance from the cameras and light sources, the results from section III.iii show clearly that those calibration parameters can not be generalized to other species and they have to be calibrated separately to obtain accurate chlorophyll concentration predictions from the NDVI values. However the good results in III.i suggest that similarly good results can be achieved for other species too.

One limiting factor in making those calibrations however is the heterogenous distribution of chlorophyll in the leaves, leading to a wide variation of NDVI values over a small ROI. This makes it hard to measure SPAD and NDVI value at exactly one point and is the reason, why we measured each point four times for the calibration.

What remains to be explained is the fact, that for SPAD values over 35 the prediction of SPAD values using the NDVI values as well as the prediction of chlorophyll concentrations from the SPAD values works considerable worse, than for smaller SPAD values. The Hypothesis that the SPAD-503 meter tends to give worse results for thicker leaves, i.e. cassava leaves with higher SPAD indexes, could not be confirmed. Neither in other more detailed research as done by John Markwell and Mitchell [4]

and Sims and Gamon [13], nor with our own data, see A.ii.

We could not gather enough data to make a definitive statement about the usefulness of the R/G data. Hence it is left for another paper to find out, whether the R/G ratios as they are calculated and displayed are good for estimating the anthocyanin concentration in the leaf. As shown by Sims and Gamon [13, page 345 et seq.] the prediction of chlorophyll concentration can be improved by taking into account anthocyanin concentrations and vice versa.

The fact that the stereoSGBM algorithm fails to produce usable disparity maps for too high plants, i.e. too high disparity values, gives us another restriction in the plant height that can be analyzed.

Further improvements of our PlantAnalyzer can be made, by choosing better Wavelengths for the IR LEDs. As can be seen in Figure 1 the Wavelength of our IR LEDs is a too high and almost in the range of the water absorbtion band [3]. A wavelength of about 800 nm may yield better results for the NDVI values. On that same note it is of course also possible to add even more LEDs with narrow emission spectra – like the Red LEDs used have – to obtain truly multispectral images. Although this has not been an issue so far, one could then also increase the image acquisition speed by applying using the LEDMSI system described by Shresta and Hardeberg [12, page 108].

V. ACKNOWLEDGEMENTS

We have to thank the following people and institutions who made this research possible and as frugal, as it was:

Evan Hutomo E. P for sharing his work and experiences with building the Low-Cost Chlorophyll Meter based on similar principles.

The DAAD (the German Academix Exchange Service) and its "RISE worldwide" internship programme which sponsored my (Jan Lukas Bosses) two month long stay in Indonesia and enabled me to do my research here.

REFERENCES

- [1] Jan Lukas Bosse. *PlantAnalyzer*. <https://github.com/mrcpp-machung/PlantAnalyzer>. 2016.
- [2] D. E. Bottrill, J. V. Possingham, and P. E. Kriedemann. "The effect of nutrient deficiencies on photosynthesis and respiration in spinach". In: *Plant Soil* 32.1-3 (1970), pp. 424–438. URL: <http://dx.doi.org/10.1007/BF01372881>.
- [3] Joseph A. Curcio and Charles C. Petty. "The Near Infrared Absorption Spectrum of Liquid Water". In: *Journal of the Optical Society of America* 41.5 (1951), p. 302. URL: <http://dx.doi.org/10.1364/JOSA.41.000302>.
- [4] John C. Osterman John Markwell and Jennifer L. Mitchell. *Calibration of the Minolta SPAD-502 Leaf Chlorophyll meter*. Tech. rep. Departments of Biochemistry, Agronomy, and School of Biological Sciences, University of Nebraska, 1995, pp. 467–472.
- [5] Johan Kjeldahl. *Zeitschrift für analytische Chemie*. Zeitschrift für analytische Chemie Bd. 22. J. F. Bergmann, 1883. URL: <https://books.google.co.id/books?id=6ePmAAAAMAAJ>.
- [6] Hartmut K. Lichtenthaler. "[34] Chlorophylls and carotenoids: Pigments of photosynthetic biomembranes". In: *Methods in Enzymology*. Elsevier BV, 1987, pp. 350–382. URL: [http://dx.doi.org/10.1016/0076-6879\(87\)48036-1](http://dx.doi.org/10.1016/0076-6879(87)48036-1).
- [7] Donald C. Rundquist Mark R. Steele Anatoly A. Gitelson and Mark N. Merzlyak. "Non-destructive Estimation of Anthocyanin Content in Grapevine Leaves". In: *Papers in Natural Resources* 283.283 (2009), pp. 87–92.
- [8] Konica Minolta. *Chlorophyll Meter SPAD-502 Plus*. last visited: 2016-09-27. 20016.
- [9] R.J. Porra, W.A. Thompson, and P.E. Kriedemann. "Determination of accurate extinction coefficients and simultaneous equations for assaying chlorophylls a and b extracted with four different solvents: verification of the concentration of chlorophyll standards by atomic absorption spectroscopy". In: *Biochimica et Biophysica Acta (BBA) - Bioenergetics* 975.3 (1989), pp. 384–394. URL: [http://dx.doi.org/10.1016/S0005-2728\(89\)80347-0](http://dx.doi.org/10.1016/S0005-2728(89)80347-0).
- [10] Jay Rambhia. *Disparity Maps*. <http://www.jayrambhia.com/blog/disparity-mpas>. last visited: 2016-09-10. 2013.
- [11] Jay Rambhia. *Stereo Calibration*. <http://www.jayrambhia.com/blog/stereo-calibration>. last visited: 2016-09-10. 2013.
- [12] Raju Shrestha and Jon Yngve Hardeberg. "Color and Imaging Conference". In: *Evaluation and Comparison of Multispectral Imaging Systems*. Vol. 2014. Society for Imaging Science and Technology. The address of the publisher, July 2014, pp. 107–112.
- [13] Daniel A Sims and John A Gamon. "Relationships between leaf pigment content and spectral reflectance across a wide range of species, leaf structures and developmental stages". In: *Remote Sensing of Environment* 81.2-3 (2002), pp. 337–354. URL: [http://dx.doi.org/10.1016/S0034-4257\(02\)00010-X](http://dx.doi.org/10.1016/S0034-4257(02)00010-X).
- [14] Compton J. Tucker. "Red and photographic infrared linear combinations for monitoring vegetation". In: *Remote Sensing of Environment* 8.2 (1979), pp. 127–150. URL: [http://dx.doi.org/10.1016/0034-4257\(79\)90013-0](http://dx.doi.org/10.1016/0034-4257(79)90013-0).

A. APPENDIX

i. Additional Calibration Results

To further check the validity of our linear models we also tested the normality of the residual (*predicted value – measured value*) values. The residual plots are show in Figure 10-15 and the results of the normality check using `scipy.stats.normaltest` are shown in Table 3

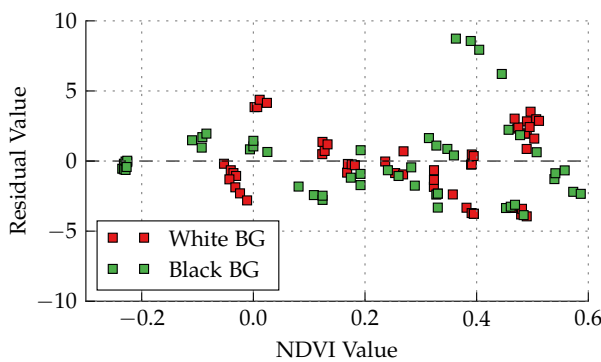


Figure 10: Plot of the Residual values of the calibration data and the dependence of the residuals on the NDVI value. Compare Figure 5

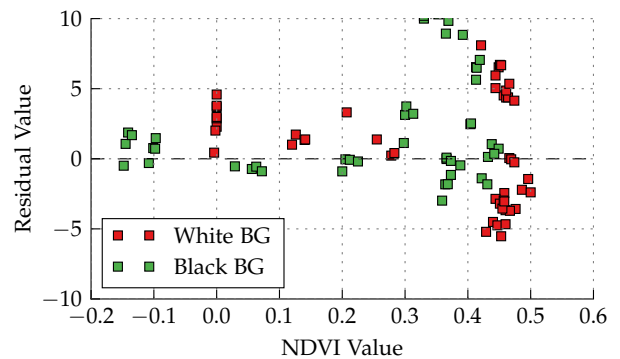


Figure 12: Plot of the Residual values of the verification data and the dependence of the residuals on the NDVI value. Compare Figure 6

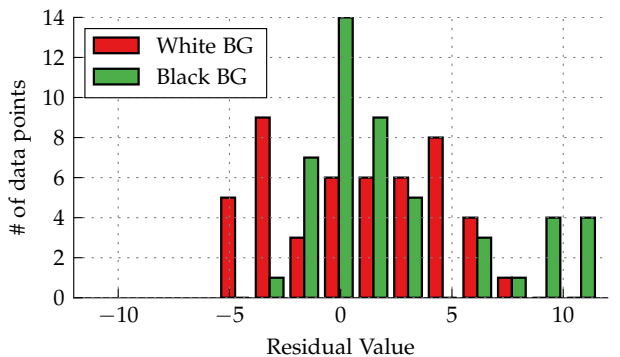


Figure 13: Histogram of the residuals of the verification data

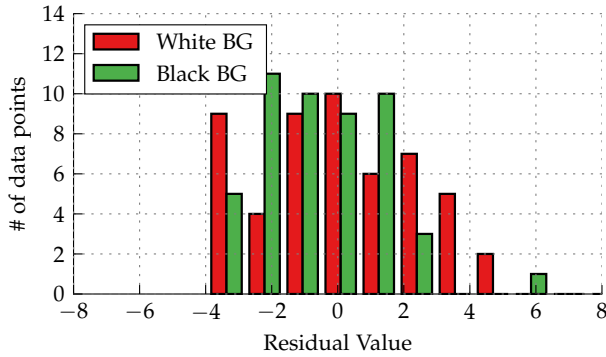


Figure 11: Histogram of the residuals of the calibration data

In the figures above one can clearly see that residuals get bigger with bigger SPAD values, in both cases, the calibration against the NDVI values and the calibration against the chlorophyll concentration values obtained from *in vitro* analysis.

The *p*-values and statistic values show clearly, what one could assume after seeing the plots of the residual values and their histograms: Except

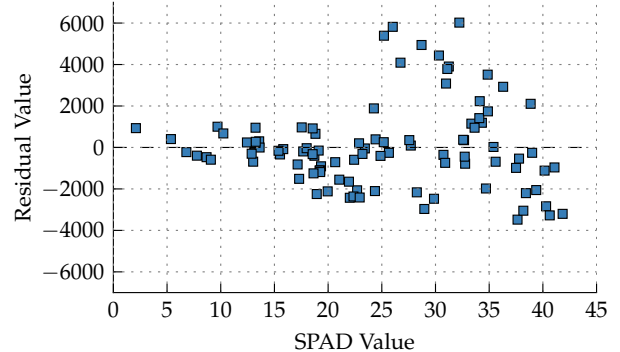


Figure 14: Residual Values of the calibration of the SPAD values to chlorophyll concentration. Compare Figure 7

for the residual values from the calibration data against a white background none of them are normally distributed.

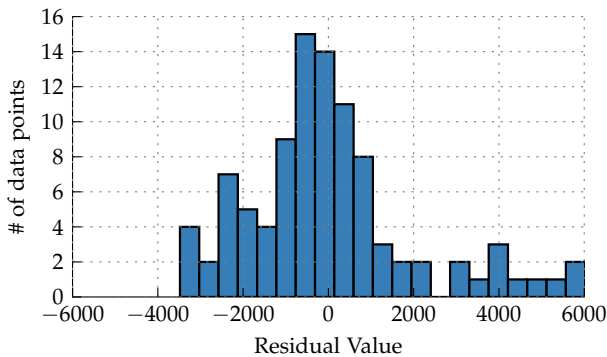


Figure 15: Histogram of the residual values in Figure 14

	statistic	p-value
calibration data white	4.1	0.129
calibration data black	24.2	$5.8 \cdot 10^{-6}$
verification data white	10.8	0.0045
verification data black	9.2	0.01
SPAD calibration data	16.9	$2.2 \cdot 10^{-4}$

Table 3: Overview over the results of the normality test of the residuals. statistic = $s^2 + k^2$ where s is the z-score returned by `skewtest` and k is the z-score returned by `kurtosistest`. p-value is the two sided p-value for the null-hypothesis that the residuals are normal.

ii. Standard Deviation of the SPAD-502 meter at higher SPAD values

To check the hypothesis, that the SPAD-502 chlorophyll meter tends to get less accurate at higher SPAD indices with cassava leaves, we had a look at the normalized standard deviations ($\frac{\sigma}{\max \text{ value}}$) of the SPAD and NDVI values from the calibration and verification measurements. As mentioned, we measured each of the data points four times, to achieve a higher accuracy. The standard deviation was taken from these four values, assuming students t-Distribution due to the extremely small sample size. The results are shown in Figure 16.

This clearly shows, that the hypothesis, that the SPAD values get less accurate for higher SPAD values can not be proven with the data we have.

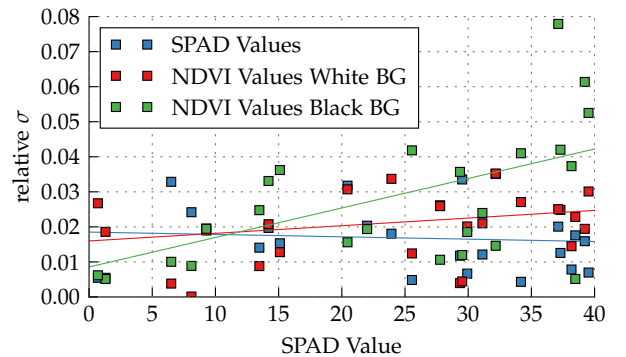


Figure 16: Normalized Standard deviations against the SPAD value.

iii. Calibration data images

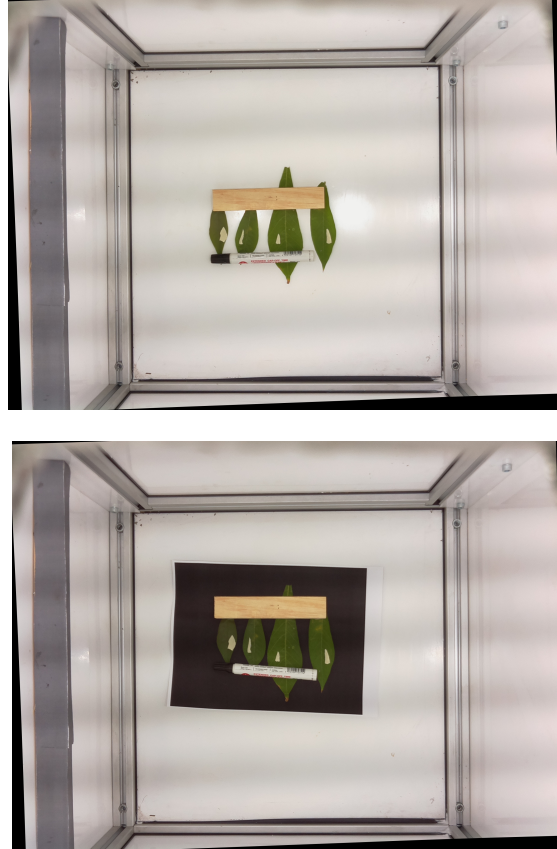


Figure 17: Four of the cassava leaves used for calibration under white illumination. Once with the white background of the analyzation chamber and once with a black piece of paper as background

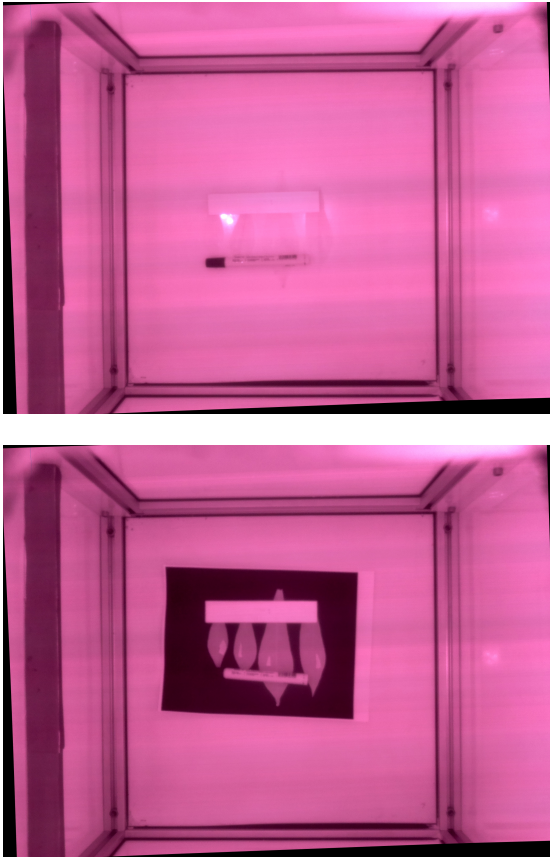


Figure 18: The same scenes as in Figure 17 under infrared illumination. It is clearly visible that the leaves with the white background have a higher radiance, than the same leaves with the black background. This means, that they are partially transparent to infrared light and thus, different calibrations for different backgrounds were needed.

iv. Calibration of the Depth Map

opencv's stereoSGBM algorithm only calculates the disparity map between two images in units of pixels. To obtain the actual distance of the object from the stereo image pair, or the area per pixel – which is obviously directly related to the former – a calibration is needed.

To obtain this calibration curve we took a stereo image pair of five checkerboards in different well defined distances from the stereo camera pair and with well defined areas. Then we calculated the disparity map using opencvs stereoSGBM algorithm. For each of the checkerboards the average dispar-

ity value was calculated and plotted against the area per pixel of this checkerboard, which was calculated by dividing the area of the checkerboard by the number of pixels it spanned in the picture.

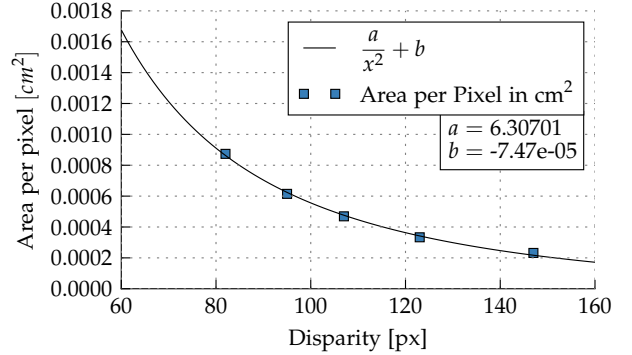


Figure 19: Calibration curves for the depth map

The result is shown in Figure 19 together with the fit parameters for a curve of the form $y = \frac{a}{x^2} + b$. We chose this curve, because it almost perfectly hit all data points and makes geometrical sense, assuming that the disparity value is linearly correlated to the distance. Hence it should allow for good area per pixel values for all other disparity values by interpolation. Extrapolation is not needed, because the five checkerboards spanned the full in the chamber possible range of distances from the stereo camera pair.

v. Flickering correction

Due to the way CMOS sensors work³ they produce bars of different brightness, if the brightness of the scene changes within the exposure time. Since we have exposure times in the order of magnitude of 1/50 s this poses a problem for us, as can be easily seen on Figure 20(a).

However since all pixels of a line are dimmed by the same fraction compared to the whole image, knowing the error of just one pixel per line allows us to correct the whole image. Assuming that the flickering of the light source scales the pixel brightness of all pixels in one line by the same

³All the lines of the image are read seperately in fast succession, leading to problems like ours or the rolling shutter effect.



(a) The uncorrected image with the flickering from the light source



(b) The corrected image. Take note of the perfectly uniformly lit calibration bar

Figure 20: While our deflickering algorithm introduces more flickering on particularly bright regions, it is far less pronounced on the leaves after deflickering. The green lines mark the column, whose brightness offsets were used to correct the whole image. This is not the full picture as taken by the Raspberry Pi cameras, but was for demonstration purposes cropped to the interesting regions

linear factor, the correction of the whole image consists simply of finding that factor and dividing pixel values of all lines by their corresponding factor. To find these factors a bar with ideally uniform reflectance was built into the analyzation chamber. (See Figure 20(b) and 20(a) on the left side). The average brightness value of pixels along the green marked column was calculated and after some denoising the ratio $\frac{\text{single pixel brightness}}{\text{average pixel brightness}}$ was used as the aforementioned factor.

Unfortunately it is not as easy, as described and the offset of each pixel from a "normalized value" does not linearly depend on its brightness, proba-

bly due to the way the picamera module internally applies non-linear tonal response curves to the raw data. Nevertheless the result after "deflickering" is still significantly better than before. Compare Figure 20(b) and 20(a).

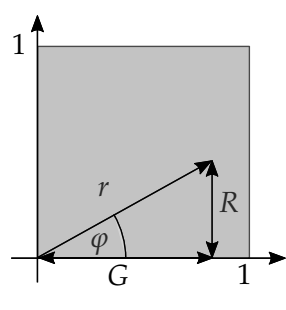
vi. Red/Green Ratio histogram equalization

Since the ratios of the red and the green channels may take values between 0 and $+\infty$ but half of them are found in the interval $[0, 1]$ – assuming the values for the red and the green channels are distributed evenly – simply rounding the resulting values to the nearest integer and then displaying the result as a heatmap does not yield usable results. The histogram has to be equalized, such that R/G ratios have an even histogram.

In order to find the right histogram equalization function we first have to find the *probability density function (PDF)* of the R/G ratios. To make things simpler, we assume that the histogram of the red and the green values is already even, and the channels are uncorrelated. I.e. the probability distribution functions are constant:

$$pdf_G(G) = pdf_R(R) = 1 \forall (R, G) \in [0, 255]^2$$

That means all value pairs of red and green values have the same probability of occurring. In the following a fixed R/G ratio $\frac{R}{G}$ will be denoted by c and the PDF of those ratios by $p(c)$.



$$\begin{aligned} G &= r \cos(\varphi) \\ R &= r \sin(\varphi) \\ \Rightarrow dG \, dR &= r \, dr \, d\varphi \\ \tan(\varphi) &= \frac{R}{G} =: c \\ \Leftrightarrow \varphi &= \arctan(c) \\ \Rightarrow d\varphi &= \frac{1}{c^2 + 1} \, dc \end{aligned}$$

Figure 21: Some geometrical considerations for the derivation of the correct histogram equalization function. Note that the interval $[0, 255]^2$ has been rescaled to $[0, 1]^2$, because this yields exactly the same results, but is more easier to calculate

As for any proper probability density function the integral over the whole domain must be the same as the number of occurring events, i.e. different value pairs of red and green reflectances. Hence

$$\int_{[0,1]^2} \underbrace{pdf_G(G) pdf_R(R)}_{=1 \text{ by assumption}} dR dG = \int_0^{+\infty} p(c) dc$$

Using the geometrical considerations from Figure 21 we will now transform the left hand side into the right hand side, until we obtain the desired $p(c)$.

$$\begin{aligned} 1 &= \int_{[0,1]^2} 1 dR \cdot dG \\ &\stackrel{\text{polar coordinates}}{=} \int_0^{\pi/2} \int_0^{\frac{1}{\cos(\varphi)}}; \varphi \leq \pi/4 r dr d\varphi \\ &\stackrel{\varphi}{=} \int_0^{+\infty} \int_0^{\frac{1}{\cos(\arctan(c))}}; c \leq 1 \frac{r}{1+c^2} dr dc \\ &\stackrel{\text{integrating over } r}{=} \int_0^{+\infty} \begin{cases} \frac{1}{2} \frac{1}{1+c^2}; c \leq 1 \\ \frac{1}{2} \frac{1}{1+c^2}; c > 1 \end{cases} dc \\ &\stackrel{\text{trigonometric identities}}{=} \int_0^{+\infty} \begin{cases} \frac{1}{2}; c \leq 1 \\ \frac{1}{2c^2}; c > 1 \end{cases} dc \\ &\quad \underbrace{p(c)}_{p(c)} \end{aligned}$$

In the last step we used that

$$\frac{1}{\cos(\arctan(c))} = \sqrt{1+c^2}$$

and

$$\frac{1}{\sin(\arctan(c))} = \frac{\sqrt{c^2+1}}{c}$$

Now that we have the PDF our histogram equalization transformation is simply the corresponding *cumulative distribution function*, i.e. its primitive times 255, to make sure we use the full range of values available to us:

$$x \mapsto \begin{cases} \frac{255 \cdot x}{2}; x \leq 1 \\ 255 - \frac{255}{2 \cdot x}; x > 1 \end{cases}$$

After this transformation we apply a logistic function

$$f(x) = \frac{255}{1 - e^{-0.05 \cdot (x-128)}}$$

to the resulting values to bring out the middle values a bit more.

Note however, that all these transformations are only done to the heatmap of the R/G ratios and not to the actual values displayed in the GUI. Those are still just the ratios.

vii. Schematics

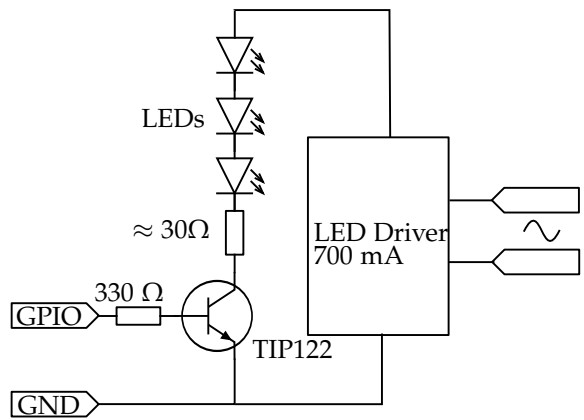


Figure 22: Scheme of the LED Control using the GPIO-Ports of the Raspberry Pi

The schematics for the LED control are shown in Figure 22. The additional 30Ω resistor was necessary, because the LED driver was specified for a output voltage of 9-11 V, but the three LEDs in series only need 6-9 V at 700 mA. Six of those controls were built for all six LED arrays.